Available online at www.sciencedirect.com
SCIENCE DIRECT®
Journal of Molecular Structure 700 (2004) 19–27
Journal of MOLECULAR STRUCTURE
www.elsevier.com/locate/molstruc

NMR studies of solid state—solvent and H/D isotope effects on hydrogen bond geometries of 1:1 complexes of collidine with carboxylic acids

Peter M. Tolstoy[a,b], Sergei N. Smirnov[b], Ilya G. Shenderovich[a,b], Nikolai S. Golubev[b], Gleb S. Denisov[b], Hans-Heinrich Limbach[a,*]

[a]*Institut für Chemie, Freie Universität Berlin, Takustrasse 3, D-14195 Berlin, Germany*
[b]*V.A. Fock Institute of Physics, St Petersburg State University, 198504 St Petersburg, Russian Federation*

Received 11 December 2003; revised 12 February 2004; accepted 13 February 2004

Abstract

^{1}H and ^{15}N NMR spectra of 10 complexes exhibiting strong OHN hydrogen bonds formed by ^{15}N-labeled collidine and different proton donors, partially deuterated in mobile proton sites, have been observed by low-temperature NMR spectroscopy using a low-freezing CDF_3/CDF_2Cl mixture as polar aprotic solvent. The following proton donors have been used: HCl, formic acid, acetic acid, various substituted benzoic acids and HBF_4. The slow hydrogen bond exchange regime could be reached below 140 K, which allowed us to resolve ^{15}N signal splittings due to H/D isotopic substitution. The valence bond order model is used to link the observed NMR parameters to hydrogen bond geometries. The results are compared to those obtained previously [Magn. Reson. Chem. 39 (2001) S18] for the same complexes in the organic solids. The increase of the dielectric constant from the organic solids to the solution (30 at 130 K) leads to a change of the hydrogen bond geometries along the geometric correlation line towards the zwitterionic structures, where the proton is partially transferred from oxygen to nitrogen. Whereas the changes of spectroscopic and, hence, geometric parameters are small for the systems which are already zwitterionic in the solid state, large changes are observed for molecular complexes which exhibit almost a full proton transfer from oxygen to nitrogen in the polar liquid solvent.

Keywords: Low-temperature NMR; Hydrogen bond; Isotope effect; Solvent effect; Collidine–carboxylic acid complex

1. Introduction

The average proton and the heavy atom positions of hydrogen bonded systems are very sensitive to electric fields [1–3]. Even small static electric field existing in solid inert gas matrixes can produce qualitative changes in the structure of hydrogen bonded complexes [4–6] or crystals by surrounding atoms or molecules. In the liquid state, large fluctuating fields arise from the dipole moments of the mobile solvent molecules. The resulting local solvation then influences strongly the average hydrogen bond complex geometry. In the case of neutral acid–base complexes, in the absence of steric hindrance between both complex constituents, in some cases a continuous change of the solvent polarity can lead to a gradual displacement of the proton from a molecular complex A–H···B to a quasi-symmetric complex $A^{\delta-}\cdots H\cdots B^{\delta+}$ [7] and eventually to a zwitterionic complex $A^{-}\cdots H{-}B^{+}$ [8,9] through the hydrogen bond center. In other cases also changes of equilibria between tautomeric forms have been observed [10,11]. In ab initio calculations, these effects can be accounted for by including static electric fields [1,2] or by polarized continuum model calculations, obtained within the Onsager or Tomasi models [12,13].

The influence of the temperature dependence of the solvent polarity on hydrogen bond geometry for small intermolecular complexes in liquid state has been studied experimentally by low-temperature NMR methods [14]. This technique has been shown to be very useful because several NMR spectral parameters, such as chemical shifts and coupling constants can be observed in the slow hydrogen bond exchange regime. Especially, ^{1}H, ^{19}F and ^{15}N NMR chemical shifts as well as homonuclear and heteronuclear scalar couplings between these spins across

* Corresponding author. Tel.: +49-30-8385-5375; fax: +49-30-8385-5310.
E-mail address: limbach@chemie.fu-berlin.de (H.-H. Limbach).

0022-2860/$ - see front matter © 2004 Elsevier B.V. All rights reserved.
doi:10.1016/j.molstruc.2004.02.023

the hydrogen bond can be observed, which are quite sensitive to the complex geometries [15–17]. Using dipolar interactions observed by solid state NMR, partially combined with data obtained from neutron diffraction or using quantum-mechanical calculations, NMR parameters were correlated with hydrogen bond distances [18–26]. These correlations were built on geometric hydrogen bond correlations observed previously by neutron crystallography, which show that a shift of the proton towards the hydrogen bond center is associated with a compression of the hydrogen bond [27]. All correlations can now be used in order to estimate hydrogen bond geometries in the liquid state by NMR [14–16,21,28,29]. However, these correlations have to be established for each system separately.

In our laboratories, in particular, hydrogen bonded complexes of pyridine-^{15}N with various acids have been studied [2,14,28,30]. In order to link the hydrogen bond geometries to the NMR parameters by dipolar solid state NMR, we tried for a long time to crystallize molecular complexes of pyridine with carboxylic acids, but were unsuccessful. However, a series of solid state 1:1 complexes between 2,4,6-trimethylpyridine (collidine) and various acids could be crystallized [31] for which solid state ^{1}H and ^{15}N NMR spectra could be obtained [23].

Therefore, in this study, we have measured the corresponding spectra of the same systems, but now dissolved in a liquid CDF_3/CDF_2Cl mixture, exhibiting a dielectric constant of between 20 at 170 K and 38 at 103 K [14]. Our goal was to establish the changes of the hydrogen bond geometries of these complexes induced by the polar solvent, as compared to the fairly non-movable solid environment, by elucidation of the ^{1}H and ^{15}N chemical shifts as well as H/D isotope effects.

2. Experimental

2.1. Materials

Commercially available substituted benzoic acids, as well as formic acid, hydrochloric acid, acetic acid and HBF_4 water solution were purchased from Aldrich. ^{15}N-enriched 2,4,6-trimethylpyridine (collidine) was synthesized from $^{15}NH_4Cl$ according to Ref. [32]. Deuteration of substituted benzoic acids was performed by repeatedly dissolving them in methanol-OD and removing the solvent under vacuum. HCl was deuterated according to the same procedure but already in complex with collidine. Formic acid, acetic acid and HBF_4 were not deuterated. Chemicals were weighed and placed into thick-walled sample NMR tubes equipped with PTFE valves (Wilmad, Buena). Collidine was added by vacuum transfer from the capillar tube connected to vacuum system. In case of HCl and HBF_4 first the complexes were synthesized, then they were weighed and added to the sample tube. The solvent, CDF_3/CDF_2Cl (freezing point below 100 K), prepared by modified method described in Ref. [33], was added to the samples by vacuum transfer. The approximate overall concentration of the samples, estimated by weighing acids and measuring the volume of the solution at low temperatures (around 120 K), was about 0.02 M.

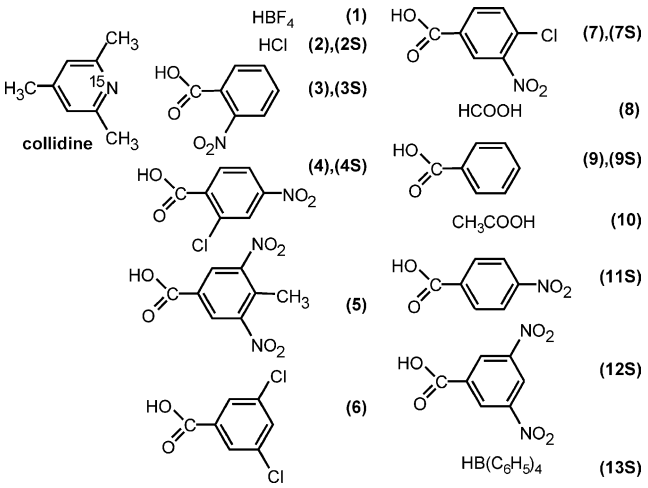

Scheme 1. Structure of 2,4,6-trimethylpyridine (collidine) and the acids studied in this paper.

2.2. NMR spectra

The Bruker AMX-500 NMR spectrometer used was equipped with a low-temperature probe-head which allowed us to perform experiments down to 100 K. ^{1}H NMR chemical shifts were measured using residual CHF_3 as internal standard, and were converted to the conventional TMS scale. The ^{15}N NMR spectra were referenced to free collidine dissolved in CDF_3/CDF_2Cl. The total deuterium fraction was determined by comparison of the integrated signal intensity of the residual mobile proton site with those of the immobile CH protons.

3. Results

The chemical structures of the acids **1**–**10** used in this study are depicted in Scheme 1. These acids can either form 1:1 or 1:2 complexes with collidine-^{15}N as illustrated in Scheme 2 in a similar way as found previously for the case of pyridine-^{15}N [30]. The low-temperature ^{1}H and ^{15}N

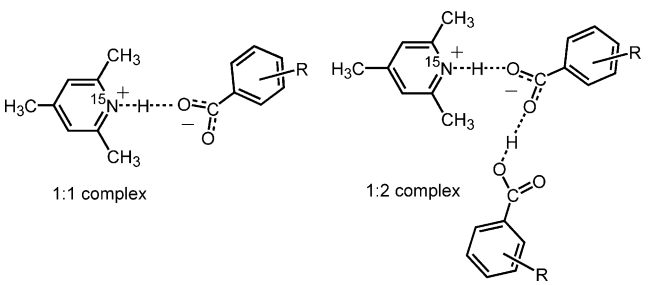

Scheme 2. Schematic representation of the structure of the hydrogen bonded 1:1 and 1:2 collidine–acid complexes in polar solution.

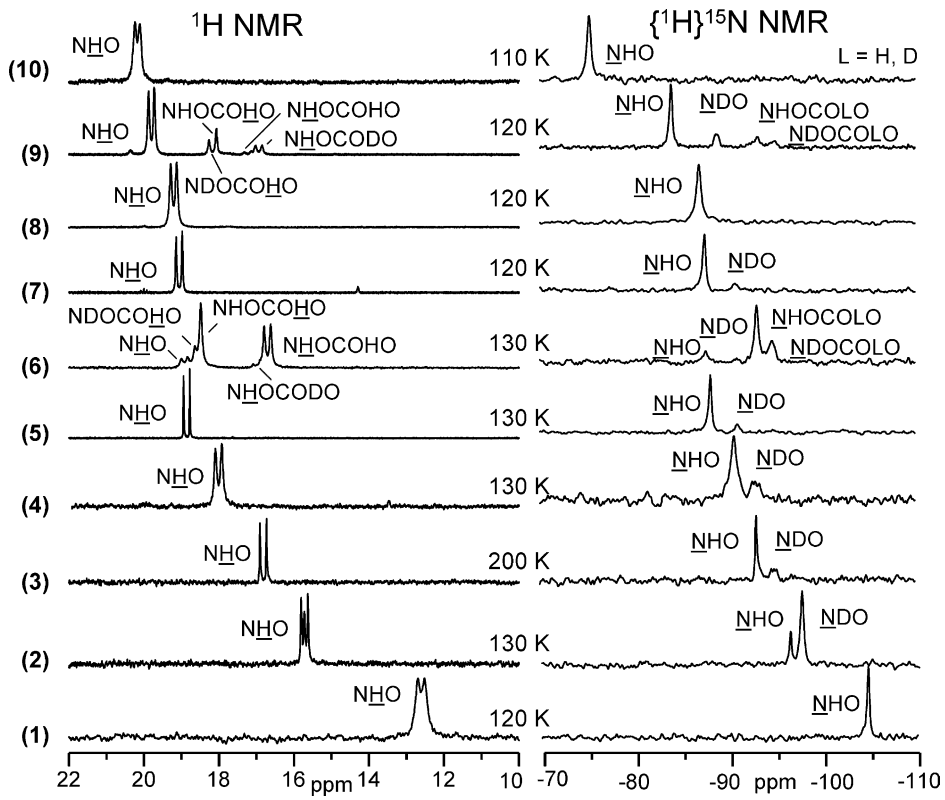

Fig. 1. Low-temperature ^{1}H and ^{15}N NMR signals of partially deuterated complexes of collidine with different proton donors in CDF_3/CDF_2Cl solution. HBF_4 (**1**), HCl (**2**), 2-nitrobenzoic acid (**3**), 2-chloro-4-nitrobenzoic acid (**4**), 3,5-dinitro-4-methylbenzoic acid (**5**), 3,5-dichlorobenzoic acid (**6**), 3-nitro-4-chlorobenzoic acid (**7**), formic acid (**8**), benzoic acid (**9**) and acetic acid (**10**). L = H, D.

signals of the solutions of collidine-^{15}N with the partially deuterated acids are depicted in Fig. 1, which also indicates the signal assignments. The N*H*O signals of 1:1 complexes are split into doublets, arising from scalar coupling with ^{15}N, characterized by the coupling constants $^1J(NHO)$. The corresponding *N*HO signals in the ^{15}N NMR spectra are singlets as {^{1}H} decoupling was employed. Because of partial deuteration, additional *N*DO signals are observed. As mentioned above, the spectra are referenced to free collidine dissolved in CDF_3/CDF_2Cl. As the deuterium fraction x_D was determined from ^{1}H spectra, the relative signal intensities in ^{15}N spectra allowed us to assign the signals to the H or D isotopologs (see Section 2 for details). We note that in the case of **2** the collidine added was enriched with ^{15}N only to about 70%, leading to a line trio, where the central line arises from the complexes with collidine-^{14}N.

In the cases of **6** and **9**, additional signals were observed arising from the corresponding 1:2 complexes. This assignment was confirmed by adding increasing amounts of acid, leading to an increase of the line intensities of the 1:2 complexes. By ^{1}H NMR the signals N*H*OCOHO,

Table 1
Experimental NMR parameters of 1:1 hydrogen bonded complexes formed between collidine and various proton donors in CDF_3/CDF_2Cl solution at low temperature

	pK_a	C_{AH}	C_B	T (K)	x_D	δ(*N*HO)	δ(*N*DO)	δ(*N*DO)−δ(*N*HO)	δ(N*H*O)	^1J(*NH*O)
HBF_4 (**1**)	< −10	0.012	0.012	120	0	−104.67			12.62	−91.9
HCl (**2**)	−7	0.022	0.022	130	0.80	−96.31	−97.52	−1.21	15.72	−89.1
2-Nitrobenzoic acid (**3**)	2.16	0.017	0.009	200	0.20	−92.63	−94.57	−1.94	16.82	−87.0
2-Chloro-4-nitrobenzoic acid (**4**)	1.96	0.013	0.014	130	0.25	−90.28	−92.65	−2.37	18.06	−84.6
3,5-Dinitro-4-methylbenzoic acid (**5**)	2.97	0.015	0.015	130	0.15	−87.77	−90.66	−2.89	18.86	−81.7
3,5-Dichlorobenzoic acid (**6**)	3.46	0.013	0.009	130	0.10	−87.27	−90.57	−3.30	18.91	−81.1
3-Nitro-4-chlorobenzoic acid (**7**)	3.66	0.020	0.024	120	0.20	−87.13	−90.42	−3.29	19.06	−80.8
Formic acid (**8**)	3.75	0.013	0.018	120	0	−86.55			19.21	−79.1
Benzoic acid (**9**)	4.19	0.088	0.070	120	0.30	−83.58	−88.44	−4.86	19.80	−76.9
Acetic acid (**10**)	4.75	0.018	0.060	110	0	−74.85			20.18	−65.4

C_{AH} and C_B, concentrations of the acid and of collidine in mol l^{-1}; x_D, deuterium fraction in the mobile proton sites; δ, chemical shifts in ppm referenced to free collidine or TMS dissolved in CDF_3/CDF_2Cl; $^1J(NHO)$, coupling constants in Hz, the sign is assumed to be negative as usual.

Table 2
Experimental NMR parameters of 1:2 complexes formed between collidine and various proton donors in CDF_3/CDF_2Cl solution at low temperature

	C_A	C_B	T (K)	x_D	δ(*N*HOCOLO)	δ(*N*DOCOLO)	δ(*N*DOCOLO)–δ(*N*HOCOLO)	δ(*NH*OCOHO)	δ(*N*HOCODO)	δ(NHOCO*H*O)	δ(NDOCO*H*O)	^1J(*NH*OCOHO)	^1J(*NH*OCODO)
3,5-Dichloro-benzoic acid (**6**)	0.013	0.009	130	0.10	−92.70	−94.32	−1.62	16.71	17.00	18.49	18.65	87.1	88.2
Benzoic acid (**9**)	0.088	0.070	120	0.30	−92.76	−94.54	−1.78	16.94	17.23	18.07	18.27	86.7	86.8

L = H, D. For further explanation see Table 1.

N*H*OCODO, NHOCO*H*O, and NDOCO*H*O are observed, where the first two signals exhibited again a scalar coupling with ^{15}N, characterized by the coupling constants $^1J(NH\text{OCOLO})$, L = H, D. Isotopic substitution in a neighbouring H-bond influences the chemical shift of a given H-bond proton, an effect which was called 'vicinal isotope effect' [34].

Deuterium fractions, chemical shifts and coupling constants for all systems studied are collected in Tables 1 and 2. The NMR data of the solid collidine-acid 1:1 complexes reported previously [23] are listed in Table 3 together with hydrogen bond distances calculated as described in the Section 4.2.

4. Discussion

4.1. NMR parameters and structure of collidine–acid complexes in CDF_3/CDF_2Cl

The spectral phenomena observed for collidine–acid complexes in CDF_3/CDF_2Cl are similar to those described previously for a series of pyridine–acid complexes [30]. When the acid is very strong, e.g. HBF_4 (**1**), typical features of a weakly or non-hydrogen bonded ion pair $A^-\cdots H{-}B^+$ are observed. They include a proton resonance $\delta(\text{NHO}) = 12.62$ ppm, a high-field ^{15}N signal at $\delta(N\text{HO}) = -104.67$ ppm with respect to free collidine dissolved in CDF_3/CDF_2Cl, and a large coupling constant $^1J(NH\text{O}) = -91.9$ Hz which is typical for this type of protonated heterocyclic systems [30,35].

When the acid becomes weaker, the proton is gradually shifted towards the anion, leading to a decrease of $^1J(NH\text{O})$ and a low-field shift of the $\delta(N\text{HO})$. During this process, the hydrogen bond contracts as indicated by the increase of the ^1H chemical shift of δ(N*H*O). Eventually, with acetic acid (**10**), a strongly hydrogen bonded quasi-symmetric complex of the type $A^{\delta-}\cdots H\cdots B^{\delta+}$ is obtained, characterized by a low-field proton signal $\delta(\text{NHO}) = 20.18$ ppm, a considerably reduced coupling constant $^1J(NH\text{O}) = -65.4$ Hz, and a value of $\delta(N\text{HO}) = -74.85$ ppm with respect to free collidine. At this point we cannot say whether the proton or deuteron moves in a double or a single well potential. This problem could be solved in the future by measuring the chemical shift of the hydrogen bond deuteron, which will be downfield for single well and upfield for double well potentials [36]. Here, we note an important difference with pyridine, where a molecular complex of the type $A{-}H\cdots B$ with acetic acid was observed, with $|^1J(NH\text{O})| < 5$ Hz, $\delta(\text{NHO}) = 17.5$ ppm and $\delta(N\text{HO}) = -27$ ppm with respect to free pyridine [30]. This difference indicates the stronger basicity of collidine, which exhibits in water a pK_a value of 7.43 at 298 K, whereas the corresponding value of pyridine is 5.32 [37].

Table 3
Experimental NMR parameters and geometric parameters of 1:1 complexes formed between collidine and various proton donors in the solid state

	Proton donors	δ^{15}N(H) (ppm)	δ^{15}N(D) (ppm)	δ^{15}N(D)−δ^{15}N(H) (ppm)	δ^{1}H (ppm)	r_{OH} (Å)	r_{HN} (Å)	q_1 (Å)	q_2 (Å)
(**2**)	HCl	−105			16.2	1.55	1.08	0.24	2.64
(**3**)	2-Nitrobenzoic acid	−95	−98	−2.8	18.3	1.43	1.12	0.15	2.55
(**4**)	2-Chloro-4-nitrobenzoic acid	−81				1.30	1.19	0.06	2.50
(**7**)	3-Nitro-4-chlorobenzoic acid	−75	−81	−6.5	18.9	1.26	1.22	0.02	2.48
(**9**)	Benzoic acid	−34	−31	3.2	14.0	1.05	1.56	−0.25	2.61
(**11**)	4-Nitrobenzoic acid	−47	−44	3.1	18.2	1.11	1.42	−0.16	2.53
(**12**)	3,5-Dinitrobenzoic acid	−89	−93	−4.0	19.7	1.37	1.15	0.11	2.52
(**13**)	$HB(C_6H_5)_4$	−120	−122	−2.4		1.89	1.03	0.43	2.92

NMR parameters from Ref. [23]. The distances are described in Section 4.2. The ^{15}N chemical shifts are referenced to neat frozen collidine.

4.2. NMR parameters and hydrogen bond geometries of collidine–acid complexes in CDF_3/CDF_2Cl

In order to compare the results obtained for liquid state with those obtained for the solid state, we have to link the ensemble of NMR parameters such as chemical shifts, coupling constants and H/D isotope effects on these parameters with the hydrogen bond geometries. As a direct determination of such geometries is not possible for the liquid state, we used for this purpose hydrogen bond correlations which have been well established [28,29]. The basis of these correlations is the experimental finding that the two distances r_{AH} and r_{HB} of a hydrogen bond AHB are not independent of each other. Thus, both distances change when the acidity or basicity of the interacting molecules are varied. This correlation is predicted by the valence bond order concept of Pauling [38]. For a hydrogen bonded system A–H···B it is assumed, that to both bonds so-called valence bond orders p_{AH} and p_{HB} can be associated whose sum is unity, i.e.

$$p_{AH} + p_{HB} = 1, \qquad p_{AH} = \exp(-(r_{AH} - r_{AH}^{\circ})/b_{AH}), \qquad p_{HB} = \exp(-(r_{HB} - r_{HB}^{\circ})/b_{HB}). \tag{1}$$

In this equation, r_{AH}° and r_{HB}° represent the distance in the free molecules AH and HB. The parameters b_{AH} and b_{HB} describe the decay of the bond orders with increasing distance. Note that the hydrogen bond angle does not enter Eq. (1), which is, therefore, independent of this angle. In the case of NHO hydrogen bonds studied here, we set A≡O and B≡N. For convenience, instead of the r_{OH} and r_{HN} we will use variables q_1 and q_2, defined as

$$q_1 = 1/2(r_{OH} - r_{HN}), \qquad q_2 = (r_{OH} + r_{HN}). \tag{2}$$

For a linear hydrogen bond q_2 corresponds to the heavy atom distance N···O and q_1 to the displacement of the proton from the hydrogen bond center. We would like to point out that for heteronuclear hydrogen bonds the geometric center does not have a particular physical meaning, as in case of homonuclear hydrogen bonded systems. An analysis of published low-temperature neutron structural crystallographic data by several authors [27] established the parameters in Eq. (1). These parameters depend slightly on the heavy atoms of the hydrogen bond as well as on the actual data set used. In a previous paper on solid collidine–acid complexes [23], some of us have used the following values for NHO hydrogen bonds

$$r_{OH}^{\circ} = 0.942 \text{ Å}; \qquad b_{OH} = 0.371 \text{ Å}; \qquad r_{HN}^{\circ} = 0.992 \text{ Å}; \qquad b_{HN} = 0.420 \text{ Å}. \tag{3}$$

By combination of Eqs. (1)–(3) the geometric hydrogen bond correlation line of Fig. 2(a) is obtained. When H is

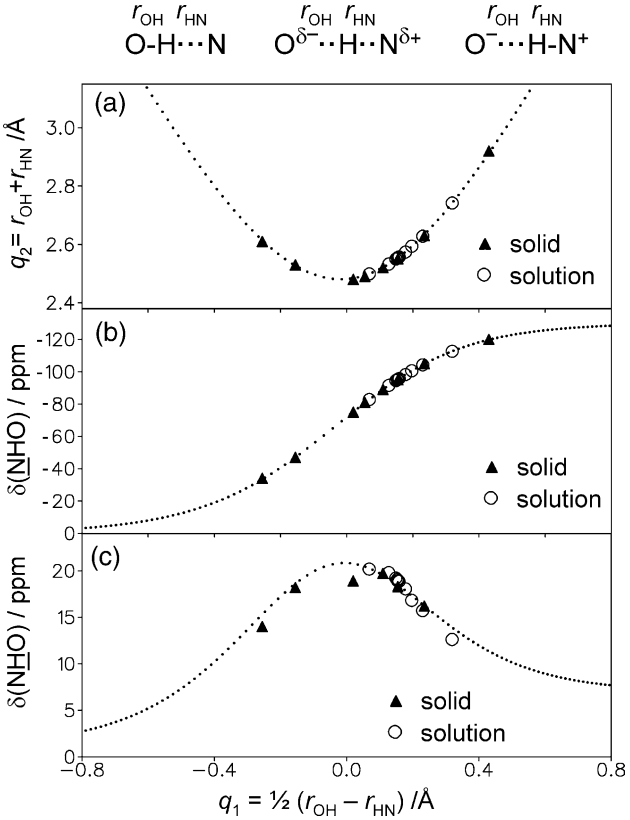

Fig. 2. Hydrogen bond correlations of collidine–acid complexes. (a) Geometric hydrogen bond correlation q_2 vs. q_1. (b) ^{15}N chemical shift correlation (Eq. (4)). (c) ^{1}H chemical shift correlation (Eq. (5)). The solid state data points are taken from Ref. [23], the liquid state data points were obtained in this study.

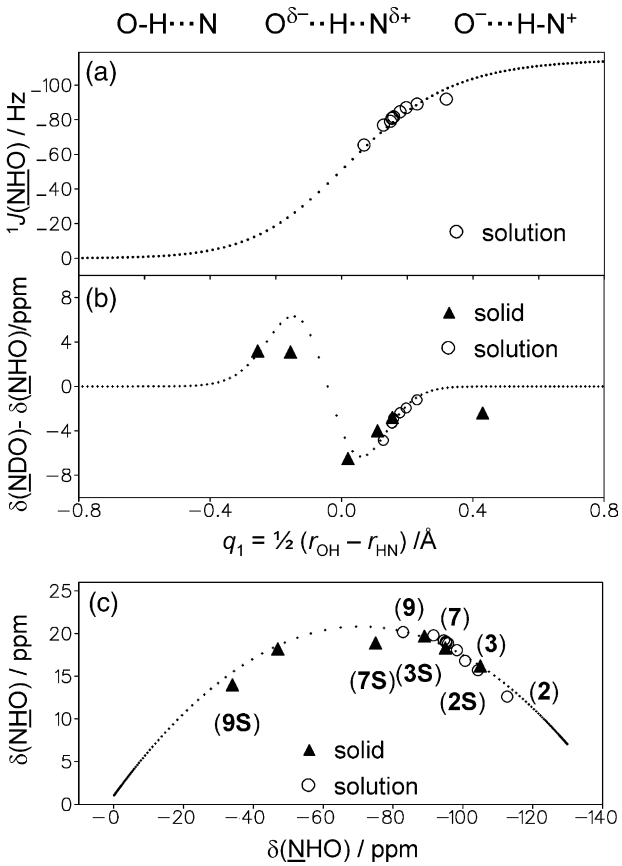

Fig. 3. Hydrogen bond correlations of collidine–acid complexes. (a) $^1J(NHO)$ coupling correlation (Eq. (6)). (b) Secondary H/D isotope effect on the ^{15}N chemical shifts. (c) δ(N*H*O) vs δ(*N*HO) correlation. For further explanation see text.

shifted from O towards N, q_2 decreases to a minimum. Once the proton has crossed the hydrogen bond center where $q_1 \approx 0$, q_2 increases again.

By measuring the dipolar ^{2}H–^{15}N coupling constant which is proportional to the average inverse cubic N···D distance r_{ND}^{-3} some of us [23] have recently established the following experimental relation between the ^{15}N chemical shifts of polycrystalline collidine–acid complexes and r_{ND} which was transformed using Eqs. (1)–(3) into the following expression

$$\delta(NHO) = \delta(N)^{\infty} - [\delta(N)^{\infty} - \delta(HN)^{\circ}]p_{HN},$$
$$\delta(N)^{\infty} - \delta(HN)^{\circ} = 130 \text{ ppm}. \quad (4)$$

$\delta(HN)^{\circ}$ and $\delta(N)^{\infty}$ are the ^{15}N chemical shifts of the fictive isolated collidinium and of free collidine. The value of full protonation shift $\delta(N)^{\infty} - \delta(HN)^{\circ} = 130$ ppm was obtained in Ref. [23] by fitting the experimental ^{15}N chemical shifts of collidine–acid complexes vs the dipolar distances r_{ND}. For a comparison of the solid and liquid state ^{15}N chemical shift data it is convenient to set the value of the neat frozen solid $\delta(N)^{\infty}$(solid) = 0. This value corresponds to 268 ppm with respect to solid $^{15}NH_4Cl$ [23], which resonates at −341.168 ppm with respect to liquid nitromethane [39]. Because of a weak hydrogen bond interaction of collidine with CDF_3/CDF_2Cl, its ^{15}N nucleus experiences a high field shift of about − 8 ppm as compared to the neat frozen state. This solvent shift could not be directly measured. Therefore, it was treated as a parameter which was varied in such a way that the liquid state ^{15}N chemical shifts could be described as well as the solid state data by Eq. (4) as using Eq. (4), the valence bond orders and hence the values of r_{OH}, r_{HN}, q_1 and q_2 were obtained for the collidine–acid 1:1 complexes in the solid state and in CDF_3/CDF_2Cl from the experimental ^{15}N chemical shifts δ(*N*HO). The results are listed in Tables 3 and 4, and the data points visualized in Fig. 2(a) and 2(b). Because of this procedure, the data points in these two graphs are located exactly on the calculated dotted correlation line.

For the ^{1}H chemical shifts correlation the following relation holds, which had been proposed previously for

Table 4
Valence bond orders and hydrogen bond geometries for acid–collidine complexes in CDF_3/CDF_2Cl

	Type	p_{OH}	p_{HN}	r_{OH} (Å)	r_{HN} (Å)	q_1 (Å)	q_2 (Å)
HBF_4 (**1**)	1:1	0.133	0.867	1.69	1.05	0.32	2.74
HCl (**2**)	1:1	0.198	0.802	1.54	1.08	0.23	2.63
2-Nitrobenzoic acid (**3**)	1:1	0.226	0.774	1.49	1.10	0.20	2.59
2-Chloro-4-nitro-benzoic acid (**4**)	1:1	0.244	0.756	1.47	1.11	0.18	2.56
3,5-Dinitro-4-methyl-benzoic acid (**5**)	1:1	0.263	0.737	1.44	1.12	0.16	2.58
3,5-Dichloro-benzoic acid (**6**)	1:1	0.267	0.733	1.43	1.12	0.16	2.55
3-Nitro-4-chloro-benzoic acid (**7**)	1:1	0.268	0.732	1.43	1.12	0.15	2.55
Formic acid (**8**)	1:1	0.273	0.727	1.42	1.13	0.15	2.55
Benzoic acid (**9**)	1:1	0.296	0.704	1.39	1.14	0.13	2.53
Acetic acid (**10**)	1:1	0.363	0.637	1.32	1.18	0.07	2.50
3,5-Dichloro-benzoic acid (**6**)	1:2	0.225	0.775	1.50	1.10	0.20	2.59
Benzoic acid (**9**)	1:2	0.225	0.775	1.50	1.10	0.20	2.60

p_{OH}, valence bond order of the OH unit; p_{HN}, valence bond order of the HN unit; r_{OH}, O···H distance; r_{HN}, N···H distance; $q_1 = 1/2(r_{OH} - r_{HN})$, $q_2 = r_{OH} + r_{HN}$ calculated according to Eqs. (1)–(4) as described in the text.

pyridine–acid complexes in Ref. [28] and supported experimentally by solid state ^{1}H NMR in the case of the solid collidine–acid complexes [23]

$$\delta(\mathrm{NHO}) = 4\Delta\delta(\mathrm{NHO})p_{\mathrm{OH}}p_{\mathrm{HN}} + \delta(\mathrm{OH})^{\circ}p_{\mathrm{OH}} + \delta(\mathrm{HN})^{\circ}p_{\mathrm{HN}}. \quad (5)$$

$\delta(\mathrm{OH})^{\circ}$ and $\delta(\mathrm{HN})^{\circ}$ represent the fictitious limiting chemical shift values of the monomeric acids and of the free pyridinium cation, and $\Delta\delta(\mathrm{NHO})$ the excess deshielding of the proton in the shortest hydrogen bond configuration. The experimental results indicated values of $\delta(\mathrm{OH})^{\circ} = 1$ ppm, $\delta(\mathrm{HN})^{\circ} = 7$ ppm, and $\Delta\delta(\mathrm{NHO}) = 16.7$ ppm leading to the dotted line in Fig. 2(c). The agreement with the experimental data is satisfactory. Of course, ^{1}H chemical shift of the OH group of free acid should be slightly different for each given acid molecule, but in Eq. (5) the value $\delta(\mathrm{OH})^{\circ} = 1$ ppm is merely a fitting parameter, which depends on the actual data set being fit. The deviation of the point near $q_1 = 0$ from the correlation curve probably indicates a larger N···O distance for a shared proton. Probably, this deviation arises from a low barrier for the proton motion. We note already now from Fig. 2, that the complexes in the liquid state are shifted on average towards the zwitterionic region as compared to the solid state. This effect will be discussed below in more detail.

For the dependence of $^1J(NH)$ coupling constants on valence bond orders in NHF bonds, an expression has been obtained [15], which is here applied for NHO bonds in the following way

$$^1J(\mathrm{NHO}) = {}^1J(\mathrm{NH})^{\circ}p_{\mathrm{HN}} - 8\Delta J(\mathrm{NHO})p_{\mathrm{OH}}^2p_{\mathrm{HN}}. \quad (6)$$

$^1J(\mathrm{NH})^{\circ}$ is the limiting coupling constant of pyridinium cation, and $\Delta J(\mathrm{NHO})$ an excess term which has to be determined experimentally. $^1J(\mathrm{NH})^{\circ}$ coupling constants for protonated pyridines can be as large as 90 Hz [30b] and unusually high value of 115 Hz in Eq. (6) is the result of the fitting procedure, similar to one done in Ref. [15], where the value of 100 Hz was obtained. Eq. (6) corresponds to the dotted line in Fig. 3(a), with the parameters $^1J(\mathrm{NH})^{\circ} = 115$ Hz, $\Delta J(\mathrm{NHO}) = 14.4$ Hz. The agreement between the experimental data and the dotted line is satisfactory, but more data are needed in order to support the parameters of Eq. (6).

For the H/D isotope effects on the nitrogen chemical shifts, the following relations have been proposed [23]. It was assumed that the valence bond order difference $\Delta p/2$ of the NHO and NDO is given by

$$\begin{aligned}\Delta p/2 &= (p_{\mathrm{DN}} - p_{\mathrm{HN}}) - (p_{\mathrm{OD}} - p_{\mathrm{OH}}) \\ &= (p_{\mathrm{OH}} - p_{\mathrm{OD}}) - (p_{\mathrm{HN}} - p_{\mathrm{DN}}) \\ &\approx A(p_{\mathrm{OH}}p_{\mathrm{HN}})^{B}(p_{\mathrm{HN}} - p_{\mathrm{OH}}), \end{aligned} \quad (7)$$

where $A = 10^4$ and $B = 7$ are empirical parameters. Eq. (7) allows one to associate to each value of r_{OH} and r_{HN}, i.e. of q_1^{H} and q_2^{H} corresponding values of r_{OD} and r_{DN}, i.e. of q_1^{D} and q_2^{D}, and hence of the H/D isotope effects on the nitrogen chemical shifts using Eq. (4). The liquid state data are in good agreement with the calculated dotted line in Fig. 3(b). Included are also the experimental values obtained for the solid state [23]. Here, the data are less precise, although the distances were derived directly from dipolar interactions, without making several assumptions, as we did during the processing of the liquid state data.

Finally, we have included in Fig. 3(c) the $\delta(\mathrm{NHO})$ vs $\delta(N\mathrm{HO})$ correlation, where the dotted line is easily obtained by the combination of Eqs. (4) and (5). We had obtained a similar curve for the complexes of pyridine with various acids in CDF_3/CDF_2Cl previously [28]. This correlation curve represents the NMR analog of the geometric correlation q_1 vs. q_2 curve of Fig. 2(a). It exhibits, however, a principal difference because the distance between the separate residues can be varied in an infinite number of ways during which their chemical shifts remain constant. Therefore, the dotted correlation line in Fig. 3(c) ends at the left and the right sides. In Fig. 3(c) we have labeled the environment of certain data points, where **S** stands for the solid state.

We observe for the collidine–acid complexes, that both the solid state as well as the liquid state data are located on the predicted dotted correlation curve in a satisfactory way. Again, we observe that the polar medium shifts the data points on the correlation line from the molecular complex towards the zwitterionic species. Note, however, that the relative order of the data points in the solid and the solution data series is preserved.

4.3. Solid state—solvent effects on the hydrogen bond geometries of collidine–acid complexes

Let us now discuss these results in a more quantitative way. Unfortunately, the two series of complexes did not overlap completely, because some of complexes studied in the solid state were not soluble in the freon mixture used. On the other hand, for certain complexes observed in the liquid state no polycrystalline powdered materials could be obtained. In order to facilitate the discussion we have plotted in Fig. 4(a) the solvent shift $\delta(N\mathrm{HO})_{\mathrm{l}} - \delta(N\mathrm{HO})_{\mathrm{s}}$ on the ^{15}N NMR chemical shifts—where the subscripts refer to l = liquid and s = solid—as a function of the hydrogen bond coordinate $q_{1\mathrm{s}}$ in the solid state. Fig. 4(b) depicts the corresponding solvent shift on the hydrogen bond coordinate $q_{1\mathrm{l}} - q_{1\mathrm{s}}$.

The origin of this transformation is the stabilization of more polar structures by the polar medium, having at 130 K a dielectric constant of about 30 [14]. The dielectric constant of the freonic mixture is subject to some changes with temperature and solvent composition, but for

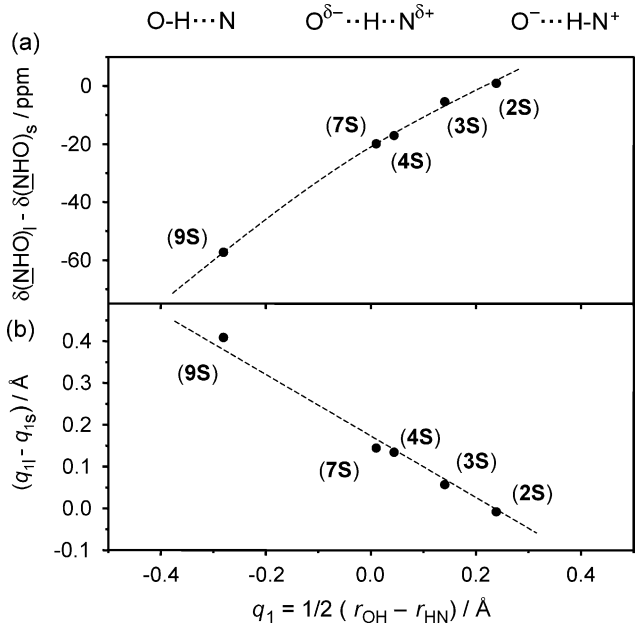

Fig. 4. Changes of the (a) ^{15}N NMR chemical shifts (subscript l = liquid, s = solid) and (b) of the hydrogen bond coordinate q_1 of complexes (**2S**), (**3S**), (**4S**), (**7S**) and (**9S**) upon the change of the environment from the crystalline state to the liquid solution in CDF_3/CDF_2Cl.

the conditions used in our work the value of ε lies in the region of 20–40. By contrast, the organic solid exhibits small dielectric constants below 5 under usual conditions. Fig. 4 demonstrates that the complexes which were already partially zwitterionic in the solid state such as **2S** show relatively small changes when they are dissolved in a polar medium. On the other hand, 'molecular' complexes such as **9S** where the proton is closer to oxygen in the solid state are particularly affected by the polar environment; they exhibit practically a full proton transfer to the base. In between these limiting cases, we observe a monotonous solid state—solution state shifts, which are almost linear as a function of q_1.

5. Conclusions

We have measured low-temperature liquid state ^{1}H and ^{15}N NMR spectra of partially deuterated 1:1 hydrogen bonded complexes of 2,4,6-trimethylpyridine (collidine) with different proton donors. A comparison of the ^{15}N chemical shifts and secondary H/D isotope effects with those obtained for the solid state shows that the high dielectric constant of the solvent (CDF_3/CDF_2Cl mixture, $\varepsilon = 20–40$) induces a proton displacement towards the nitrogen atom and formation of zwitterionic complexes, which is particularly strong for molecular complexes. The data obtained may serve in the future as test cases for quantum-mechanical calculations of acid–base complexes as a function of the polarity of the environment.

Acknowledgements

This research has been supported by the Deutsche Forschungsgemeinschaft, Bonn, the Fonds der Chemischen Industrie, Frankfurt, and the Russian Foundation of Basic Research, Grants 03-03-04009, 03-03-06504 and 03-03-32272. P.T. thanks the Fonds for a Kékulé scholarship.

References

[1] M. Ramos, I. Alkorta, J. Elguero, N.S. Golubev, G.S. Denisov, H. Benedict, H.-H. Limbach, J. Phys. Chem. A 101 (1997) 9791.
[2] J.E. Del Bene, M.J.T. Jordan, J. Phys. Chem. A 106 (2002) 5385.
[3] N.S. Golubev, G.S. Denisov, S.N. Smirnov, D.N. Shchepkin, H.-H. Limbach, Z. f. Phys. Chem. 196 (1996) 73.
[4] A.J. Barnes, Z. Latajka, M. Biczysko, J. Mol. Struct. 614 (2002) 11.
[5] L. Andrews, X. Wang, J. Phys. Chem. A 105 (2001) 6420.
[6] L. Andrews, X. Wang, Z. Mielke, J. Phys. Chem. A 105 (2001) 6054.
[7] N.V. Drichko, G.Y. Kerenskaia, V.M. Schreiber, J. Mol. Struct. 477 (1999) 127.
[8] A. Abkowicz-Bieńko, M. Biczysko, Z. Latajka, Comput. Chem. 24 (2000) 303.
[9] A.I. Kulbida, V.M. Schreiber, J. Mol. Struct. 47 (1978) 323.
[10] R. Langner, G. Zundel, J. Chem. Soc. Faraday Trans. 21 (1995) 3831.
[11] T. Kuc, Th. Zeegers-Huyskens, Z. Pawelka, J. Mol. Liquids 89 (2000) 147.
[12] J. Tomasi, M. Persico, Chem. Rev. 94 (1994) 2027.
[13] M.A. McAllister, Can. J. Chem. 75 (1997) 1195.
[14] I.G. Shenderovich, A.P. Burtsev, G.S. Denisov, N.S. Golubev, H.-H. Limbach, Magn. Reson. Chem. 39 (2001) S91.
[15] I.G. Shenderovich, P.M. Tolstoy, N.S. Golubev, S.N. Smirnov, G.S. Denisov, H.-H. Limbach, J. Am. Chem. Soc. 125 (2003) 11710.
[16] I.G. Shenderovich, H.-H. Limbach, S.N. Smirnov, P.M. Tolstoy, G.S. Denisov, N.S. Golubev, Phys. Chem. Chem. Phys. 4 (2002) 5488.
[17] N.S. Golubev, S.M. Melikova, D.N. Shchepkin, I.G. Shenderovich, P.M. Tolstoy, G.S. Denisov, Z. f. Phys. Chem. 217 (2003) 1549.
[18] U. Sternberg, E. Brunner, J. Magn. Res. A 108 (1994) 142.
[19] A. McDermott, C.F. Ridenour, in: D.M. Grant, R.K. Harris (Eds.), Encyclopedia of Nuclear Magnetic Resonance, Wiley, Chichester, 1996, p. 3820.
[20] K. Yamauchi, S. Kiroki, I. Ando, J. Mol. Struct. 602–603 (2002) 9.
[21] T.K. Harris, A.S. Mildvan, Proteins: Struct. Funct. Genet. 35 (1999) 275.
[22] H. Benedict, H.-H. Limbach, M. Wehlan, W.P. Fehlhammer, N.S. Golubev, R. Janoschek, J. Am. Chem. Soc. 120 (1998) 2939.
[23] P. Lorente, I.G. Shenderovich, N.S. Golubev, G.S. Denisov, G. Buntkowsky, H.-H. Limbach, Magn. Reson. Chem. 39 (2001) S18.
[24] A. Fukutani, A. Naito, S. Tuzi, H. Saito, J. Mol. Struct. 602–603 (2002) 491.
[25] T. Heinz, O. Moreira, K. Pervushin, Helv. Chim. Acta 85 (2002) 3984.
[26] J.E. Del Bene, Magn. Res. Chem. 40 (2002) 767.
[27] (a) T. Steiner, W. Saenger, Acta Crystallogr. B50 (1994) 348.
(b) T. Steiner, J. Chem. Soc. Chem. Commun. (1995) 1331.
(c) P. Gilli, V. Bertolasi, V. Ferretti, G. Gilli, J. Am. Chem. Soc. 116 (1994) 909.
(d) T. Steiner, J. Phys. Chem. A 102 (1998) 7041.
[28] S.N. Smirnov, H. Benedict, N.S. Golubev, G.S. Denisov, M.M. Kreevoy, R.L. Schowen, H.-H. Limbach, Can. J. Chem. 77 (1999) 943.
[29] H. Benedict, I.G. Shenderovich, O.L. Malkina, V.G. Malkin, G.S. Denisov, N.S. Golubev, H.-H. Limbach, J. Am. Chem. Soc. 122 (2000) 1979.
[30] (a) N.S. Golubev, S.N. Smirnov, V.A. Gindin, G.S. Denisov, H. Benedict, H.-H. Limbach, J. Am. Chem. Soc. 116 (1994) 12055.

(b) S.N. Smirnov, N.S. Golubev, G.S. Denisov, H. Benedict, P. Schah-Mohammedi, H.-H. Limbach, J. Am. Chem. Soc. 118 (1996) 4094.
[31] C. Foces-Foces, A.L. Llamas-Saiz, P. Lorente, N.S. Golubev, H.-H. Limbach, Acta Crystallogr. C55 (1999) 377.
[32] K. Dimroth, Angew. Chem. 10 (1960) 331.
[33] J.S. Siegel, F.A.I. Anet, J. Org. Chem. 53 (1988) 2629.
[34] C. Detering, P.M. Tolstoy, N.S. Golubev, G.S. Denisov, H.-H. Limbach, Doklady RAN 379 (2001) 353 (Engl. Ed.: Doklady Phys. Chem. 379 (2001) 191).
[35] R.O. Duthaler, J.D. Roberts, J. Am. Chem. Soc. 100 (1978) 4969.
[36] P. Schah-Mohammedi, I.G. Shenderovich, C. Detering, H.-H. Limbach, P.M. Tolstoy, S.N. Smirnov, G.S. Denisov, N.S. Golubev, J. Am. Chem. Soc. 122 (2000) 12878.
[37] D.R. Lide, CRC Handbook of Chemistry and Physics, 81 ed., CRC Press LLC, London, 2000–2001.
[38] (a) L. Pauling, J. Am. Chem. Soc. 69 (1947) 542.
(b) I.D. Brown, Acta Crystallogr. B48 (1992) 553.
(c) D. Dunitz, Philos. Trans. R. Soc. London B272 (1975) 99.
[39] S. Hayashi, K. Hayamizu, Bull. Chem. Soc. Jpn 64 (1991) 688.